Plasma Astrophysics

Toshiki Tajima, UCI

Class 8:PHY249 (2020Spring)

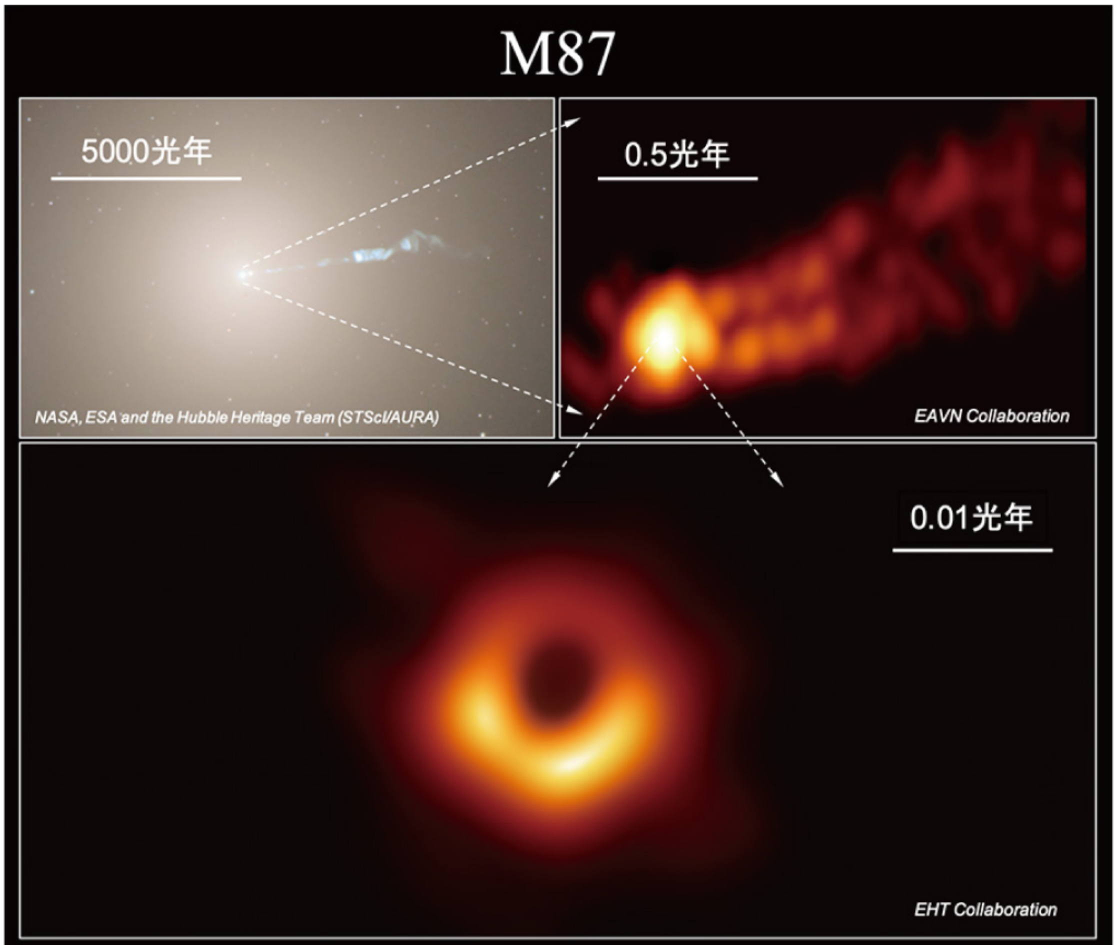

Event Horizon Telescope (2020)

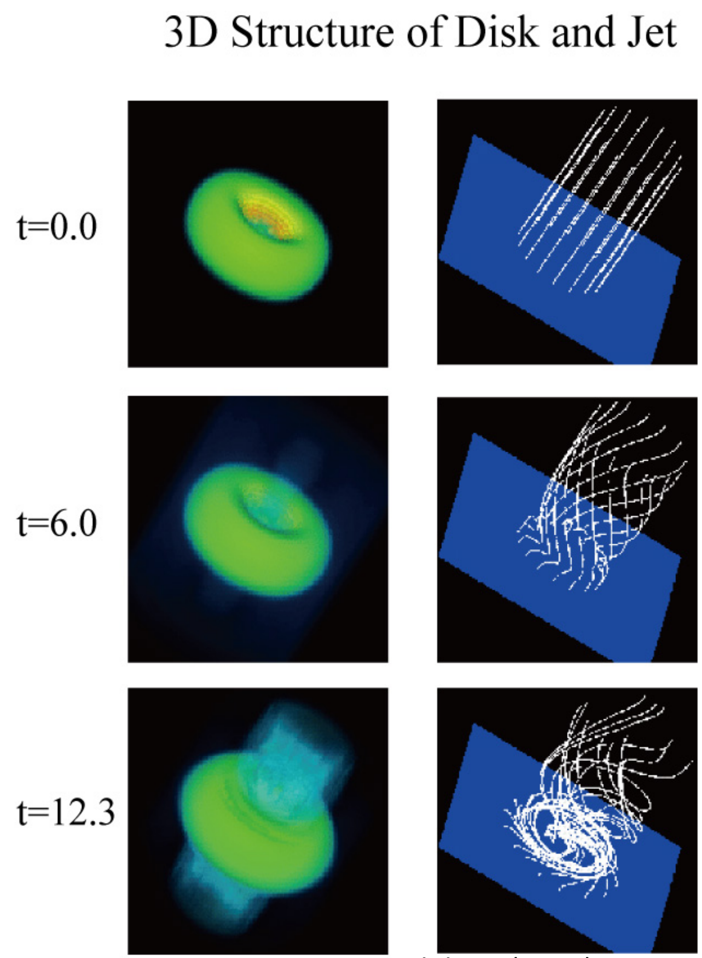

Tajima Shibata (1997) p. 387

Plasma Astrophysics (Tajima, 2020)

- Class 8: Informal suggestions for the Term Project proposals:

-**Do we have (or will have) localized UHECRs?** ←

-**What properties do they have?** ←

such as

high energies? (such as ~ or > 10^{19} eV?)

spatial localization?

time structures?

accompaniment of other waves (γ, X, radio, light)?

cosmic rays other than protons (such as neutrinos)?

-**Are they explainable by the new theory?**

Partially reorganized from Class 7 deck

Localizable Brightest cosmic rays by wakefields ?

(A)

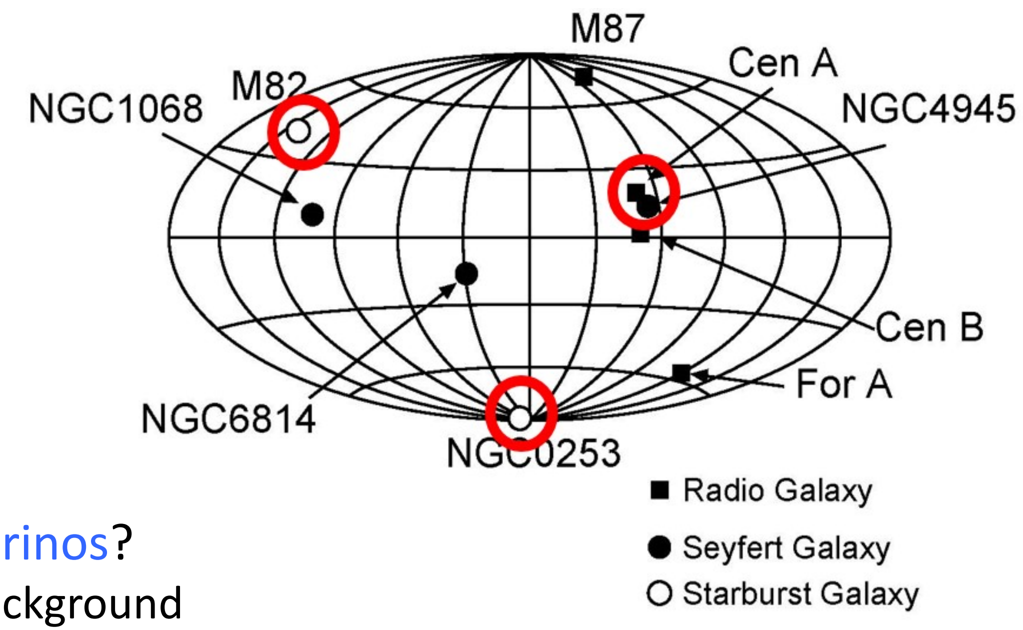

Localized UHECR?

thus Localized neutrinos?

not as a spread background

(B)

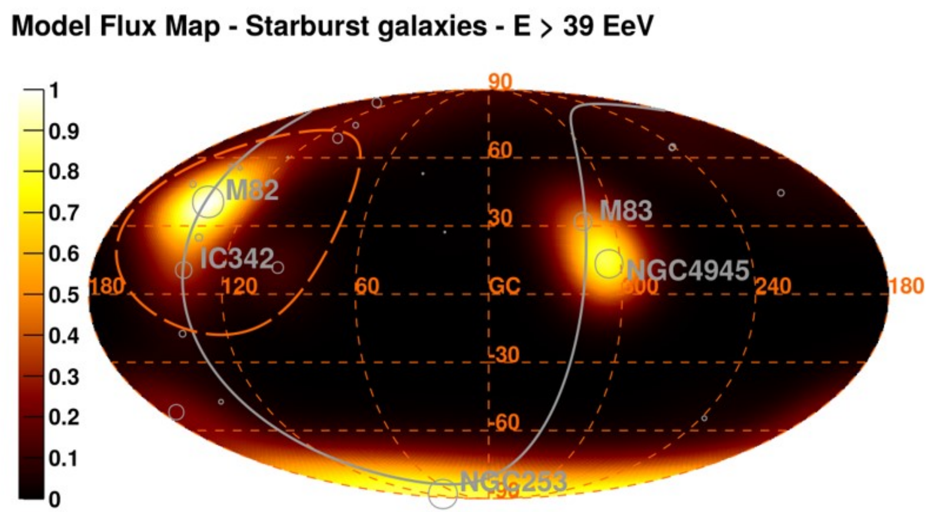

II. Specific examples ← our theory

0. Blackhole (BH) as an engine of AGN [textbook p.387]

1. Blazar γ-emmission → protons (UHECR); time-structured, coincidental with γ, neutrino

[Canac, et al. 2020;IceCube, Science, 2020]

2. M82 (starburst galaxy) [see refs. inside]

3. Cen A (radio galaxy) [see refs. inside]

4. NGC 0253 (starburst galaxy) [see refs. inside]

5. SS 433 (microquasar) [Abeysakara et al., 2018]

[other refs. are also inside of these slides]

Energy release by Wakefield (e.g.M82 X-1)

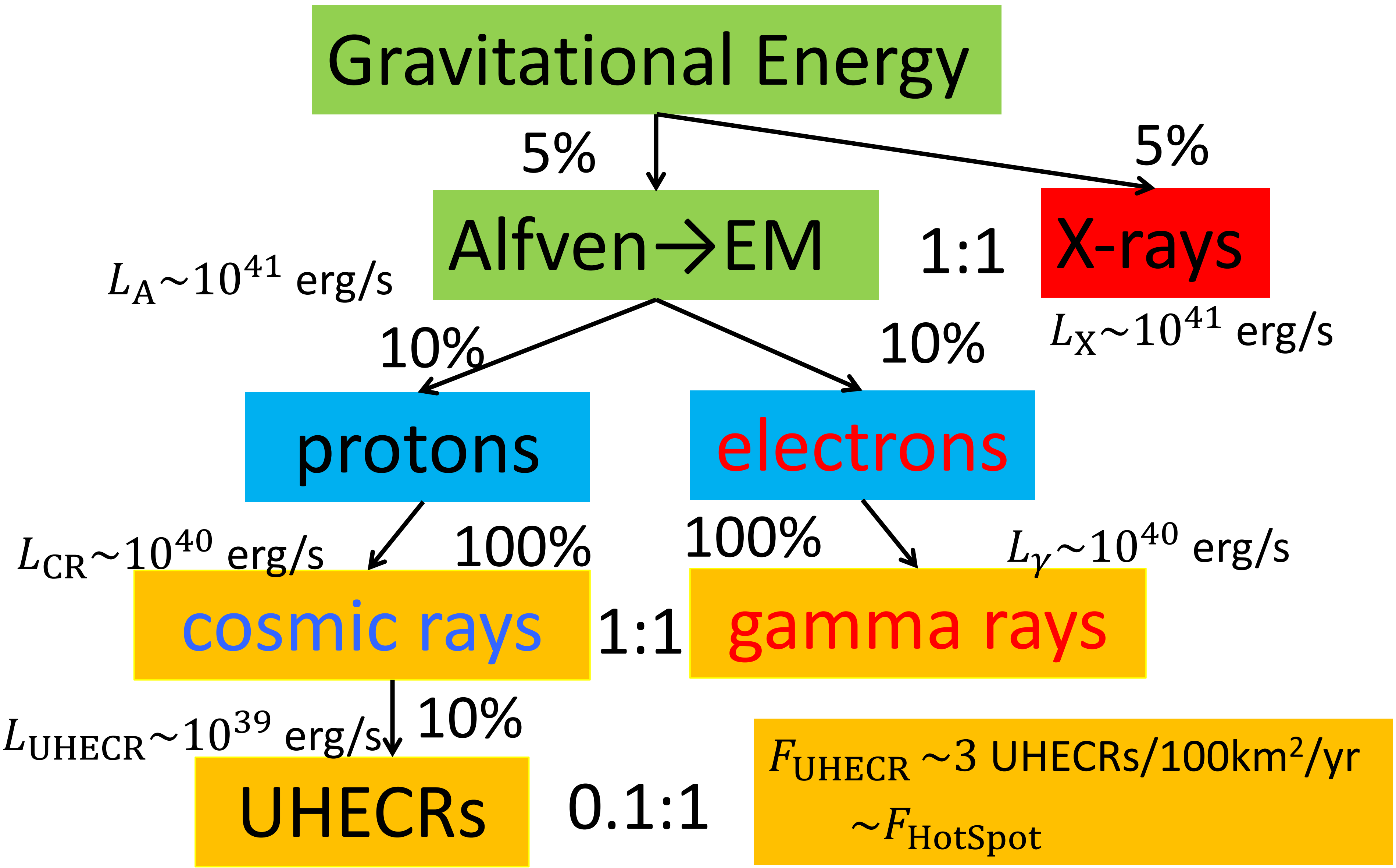

cosmic ray acceleration and gamma-ray emission

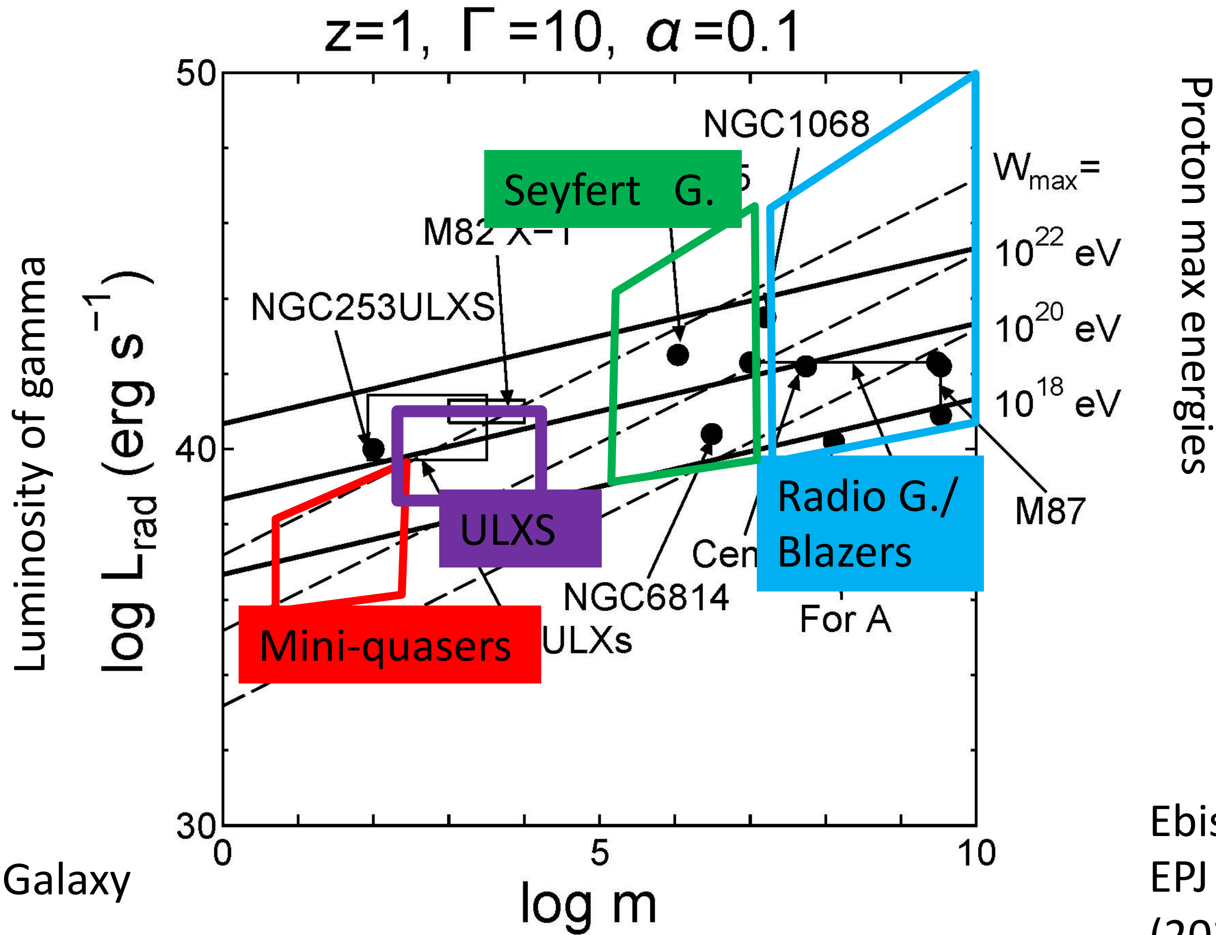

Miniquasars:
can be in our Galaxy

Ebisuzaki, Tajima
EPJ **223**, 1113(2014);
(2020)

BH Astronomy with Ultra High Energy CRs

I. Contrast of old vs. new

Prevailing theory (Fermi's stochastic acceleration; 1954)

a. energy beyond 10^{19} eV not possible

b. isotropic HECR arrival

c. No time structure

d. No expected other signals s.a. γ emissions

New Theory (Wakefield acceleration; 1979-)

not to deny the old theory, but can explain new things

A. beyond 10^{18-19} eV possible

B. localized

C. time structured

D. correlated with other signals (s.a. γ emissions, etc.)

E. non-protons (s.a. pinpointed neutrino)

Wakefields: Bow and Wake

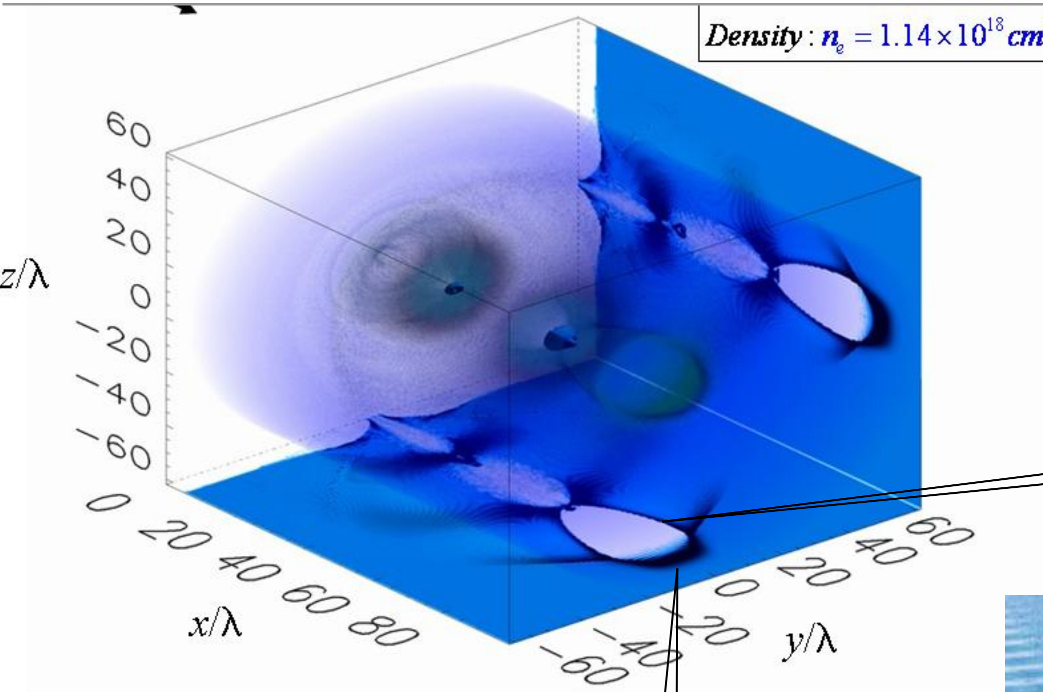

(Bulanov, Esirkepov)

Wakefield acceleration

Wake Wave

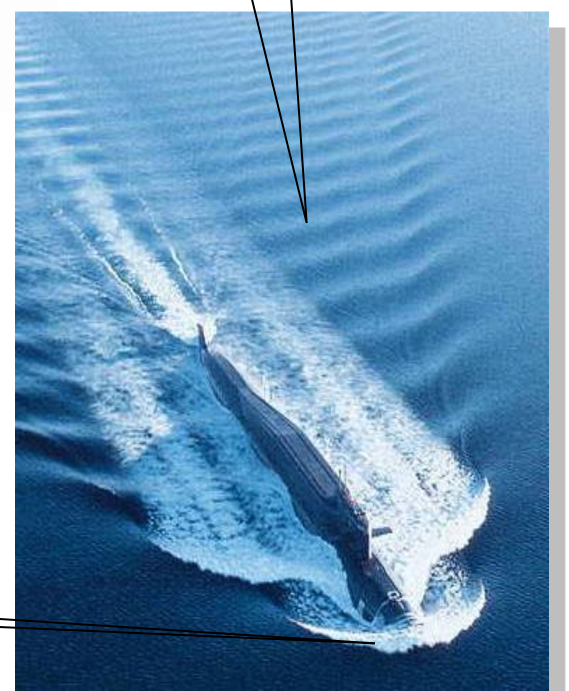

Coherent, **collective**, **robust**, **huge amplitude**

Bow Wave

Ponderomotive acceleration

wakes:

Kelvin wake

No wave breaks and wake **peaks** at v≈c

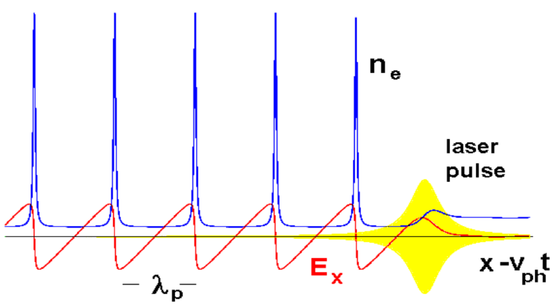

← relativity regularizes

(***relativistic coherence***)

(The density cusps.
Cusp singularity)

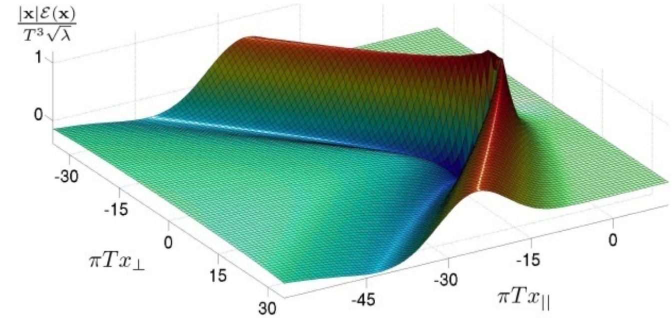

Maldacena

(Plasma physics vs. String theory)

Maldacena (string theory) method:
QCD **wake** (Chesler/Yaffe 2008)

Wave **breaks** at v<c

Hokusai

Universal Theory of Wakefield toward extreme energy

$$\Delta E \approx 2m_0c^2a_0^2\gamma_{ph}^2 = 2m_0c^2a_0^2\left(\frac{n_{cr}}{n_e}\right),$$ (when 1D theory applies)

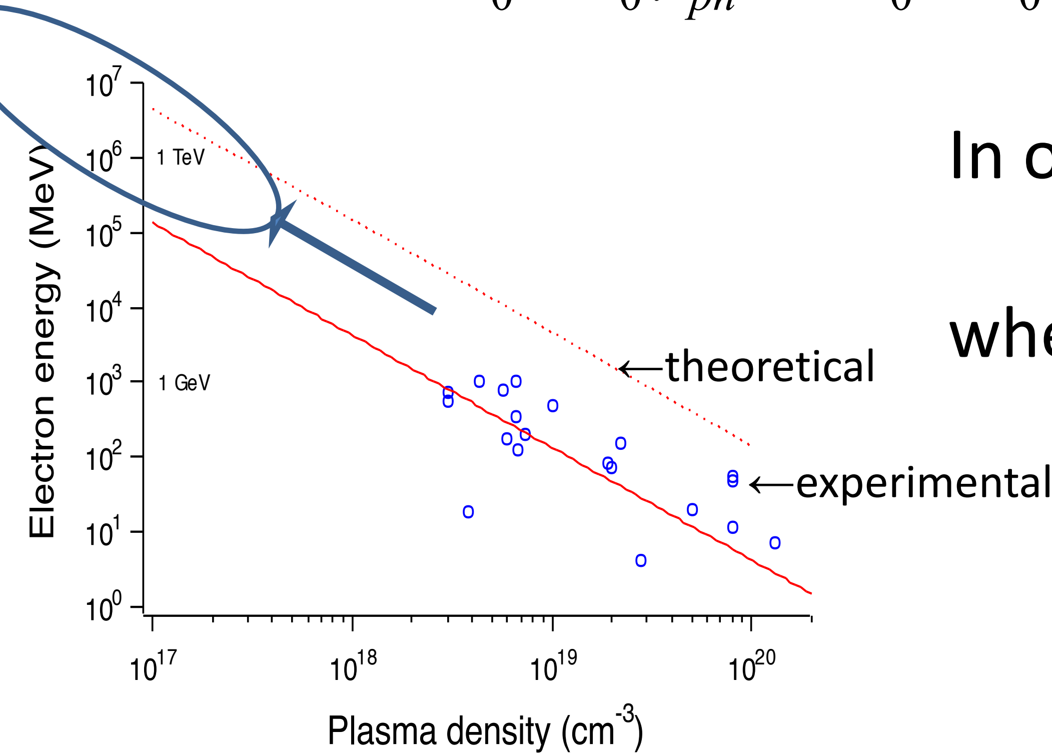

In order to avoid wavebreak,

$$a_0 < \gamma_{ph}^{1/2},$$

where

$$\gamma_{ph} = (n_{cr} / n_e)^{1/2}$$

n_{cr} =10^{21} (fs photon (laser))

= 10 (10^3 s wave in disk)

n_e = 10^{18} (gas)

= 10^{-2} (gas in the jet)

$$L_d = \frac{2}{\pi}\lambda_p a_0^2\left(\frac{n_{cr}}{n_e}\right),$$

dephasing length

$$L_p = \frac{1}{3\pi}\lambda_p a_0\left(\frac{n_{cr}}{n_e}\right),$$

pump depletion length

Electron, proton accelerators

Wakefield accelerator (GeV/cm)

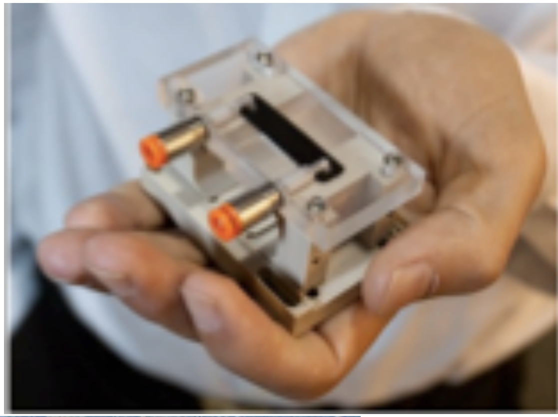

SLAC electron accelerator (10^1 GeV)

Fermilab proton accelerator (Tevatron) (10^1 TeV)

Ultrahigh Energy Cosmic Rays (UHECR)

Fermi mechanism runs out of steam
  beyond 10^{19} eV
  due to synchrotron radiation

Wakefield acceleration
  comes in rescue
  prompt, intense, linear acceleration
  small synchrotron radiation
  radiation damping effects?

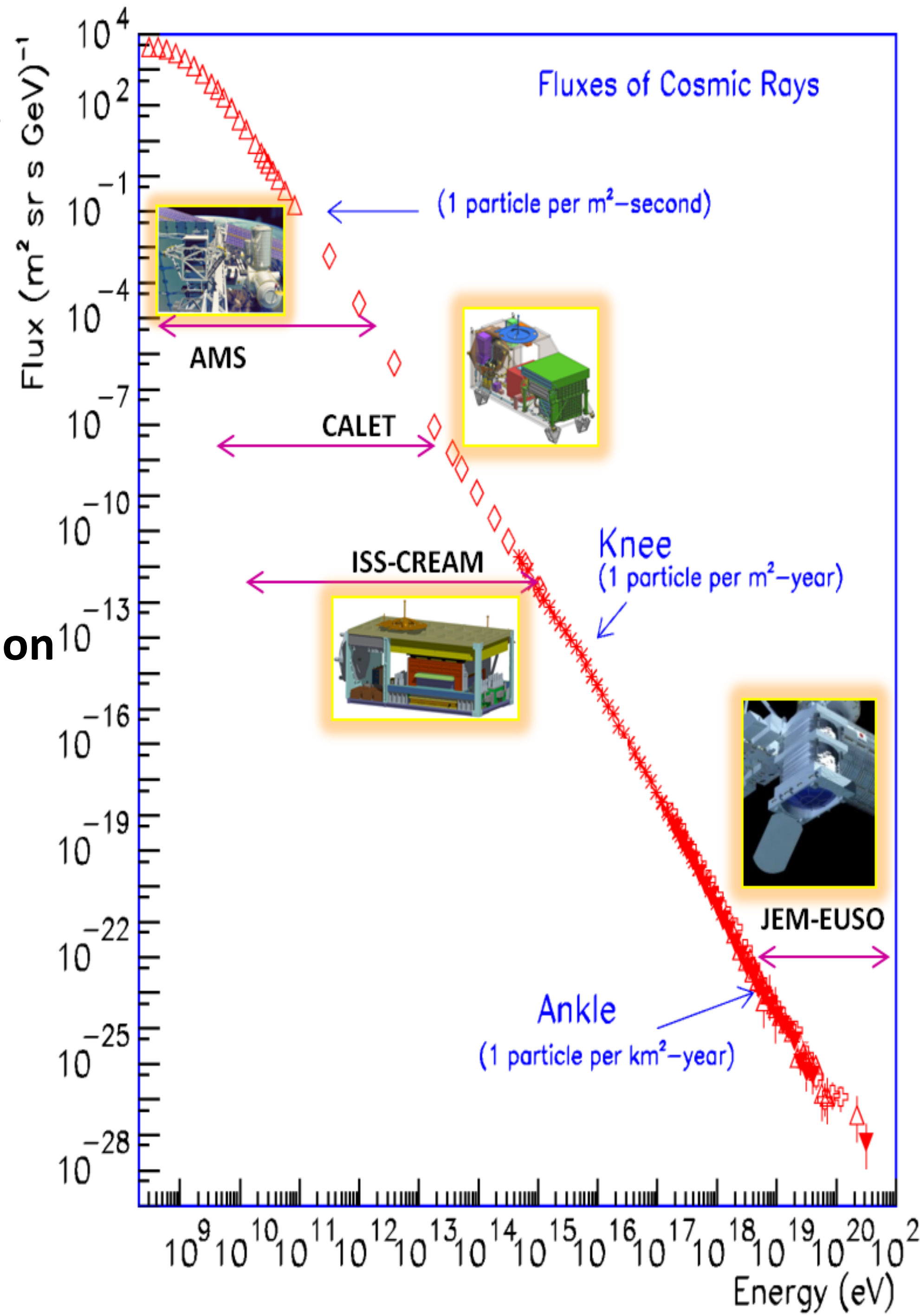

Astrophysical wakefield acceleration: Superintense Alfven Shock in the Blackhole Accretion Disk toward ZeV Cosmic Rays (a_0 ~ 10^6 -10^{10}, large spatial scale)

$a_0 = eE_0 / mc\omega_0 >> 1$: normalized EM wave amplitude

E_0: modest

$\omega_0 = 2\pi c / \lambda$: extremely low

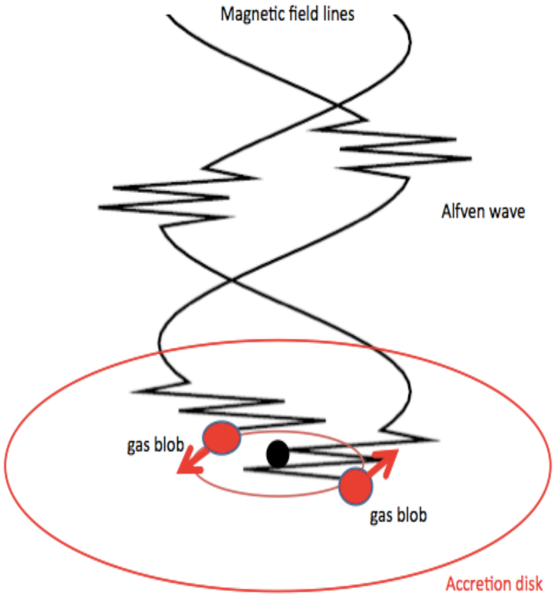

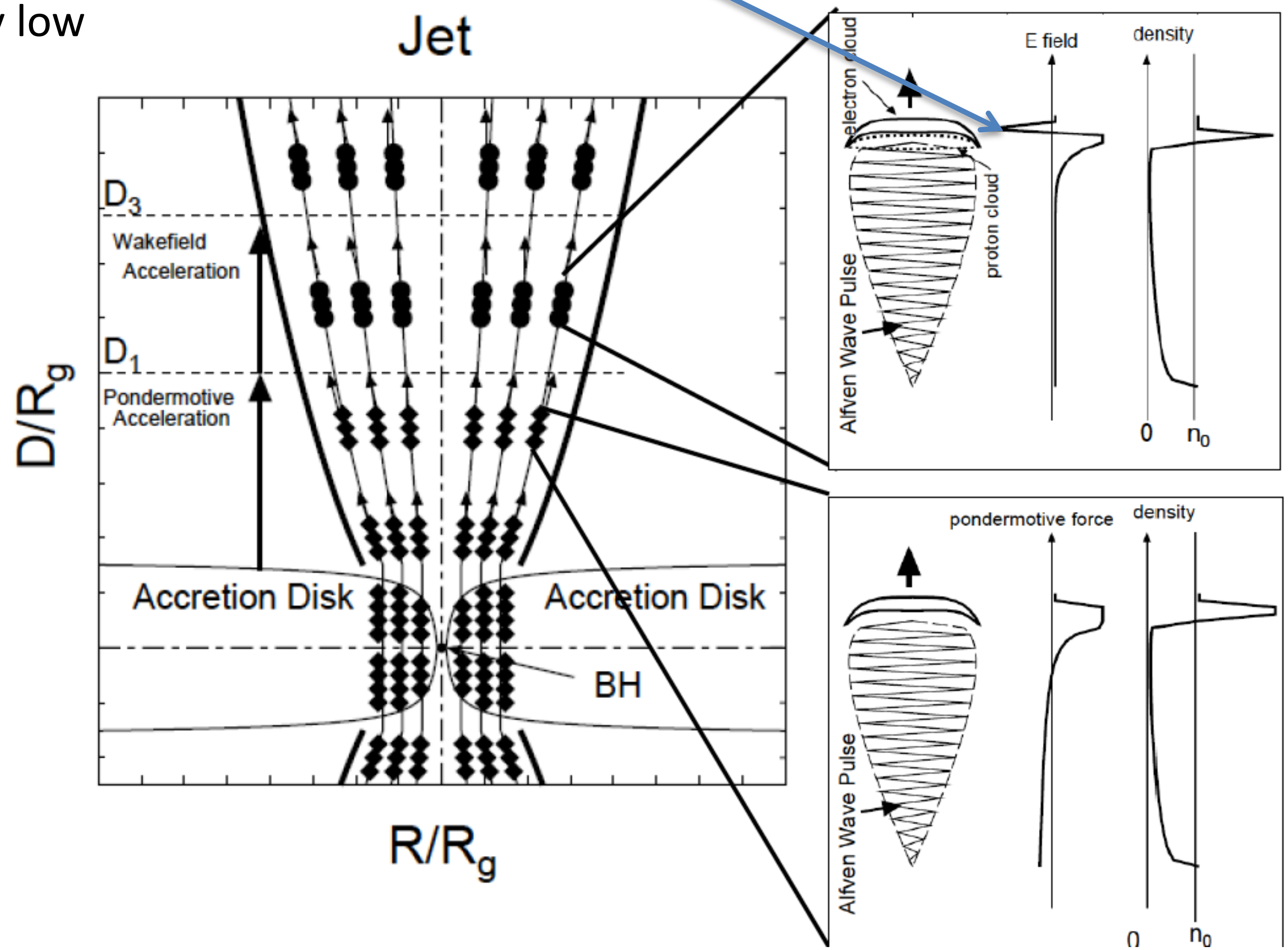

Ebisuzaki and Tajima, Astropart. Phys.(2014)

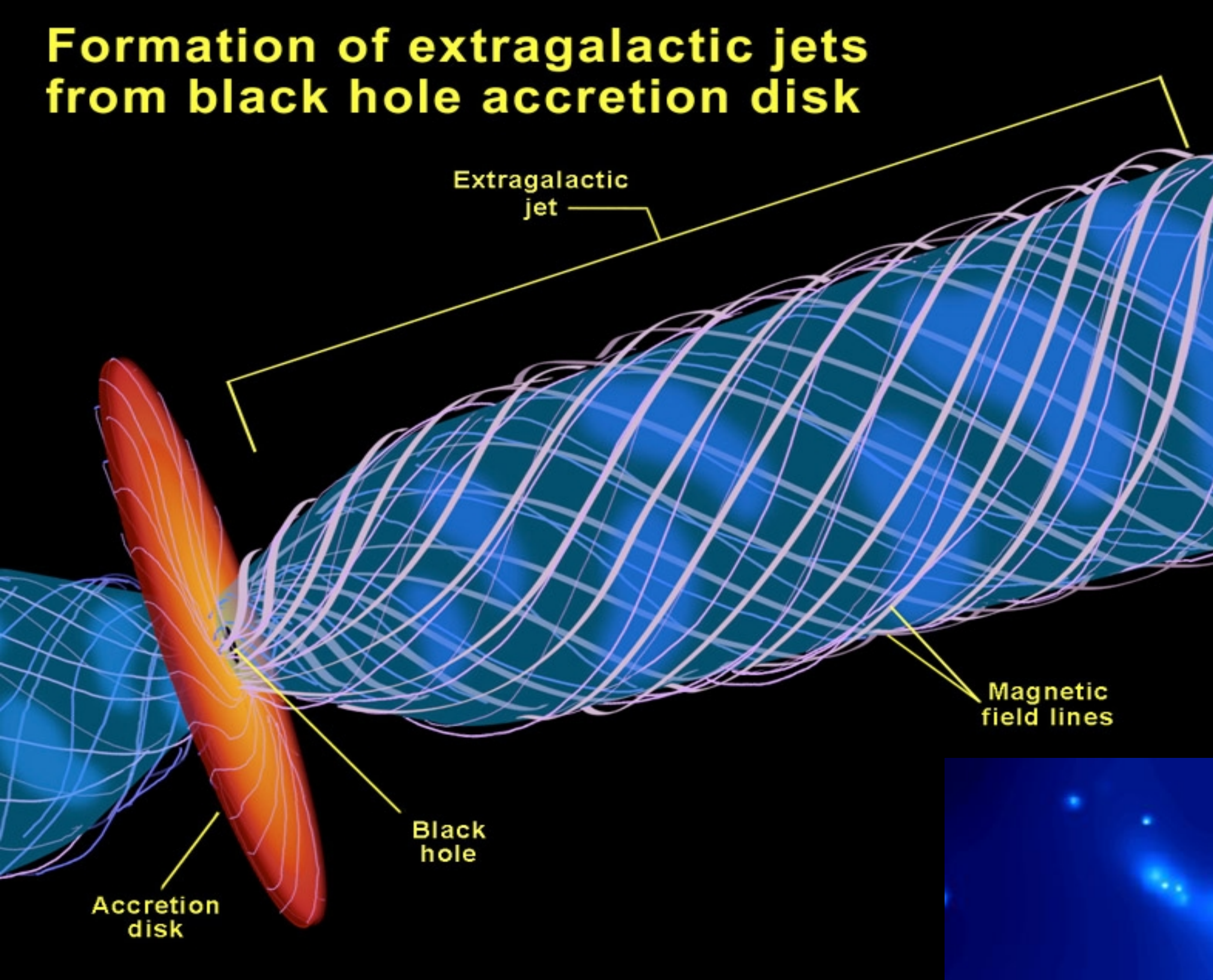

Fermi's **'Stochastic Acceleration'**
(large synchrotron radiation loss)

↓

Coherent wakefield acceleration
(no limitation of the energy)

Nature's LWFA : Blazar jets
extreme high energy cosmic rays (~10^{21} eV)
episodic γ-ray bursts observed
consistent with LWFA theory

Ebisuzaki-Tajima (2014)

Halo and jet acceleration in an accretion disk

A Burst of Electromagnetic Disturbance

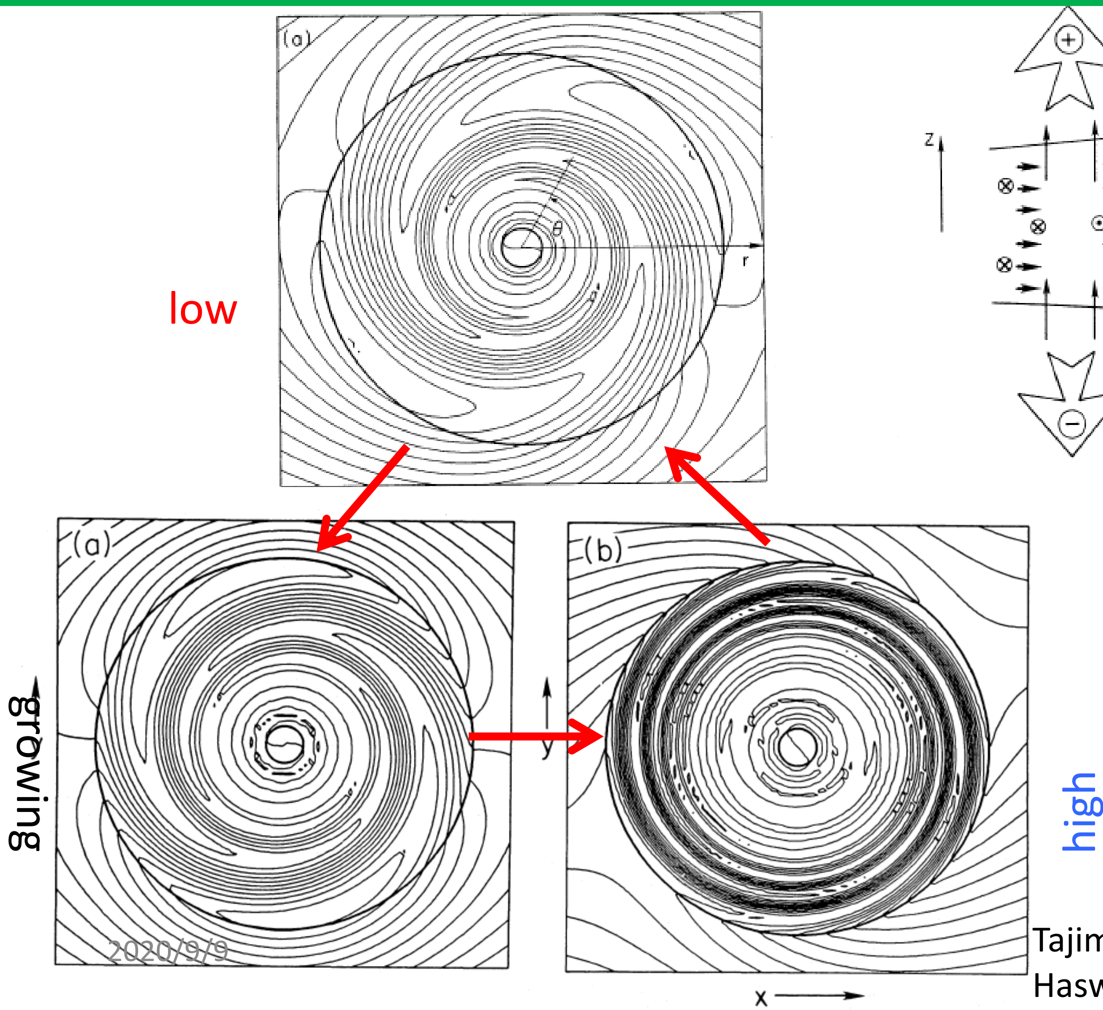

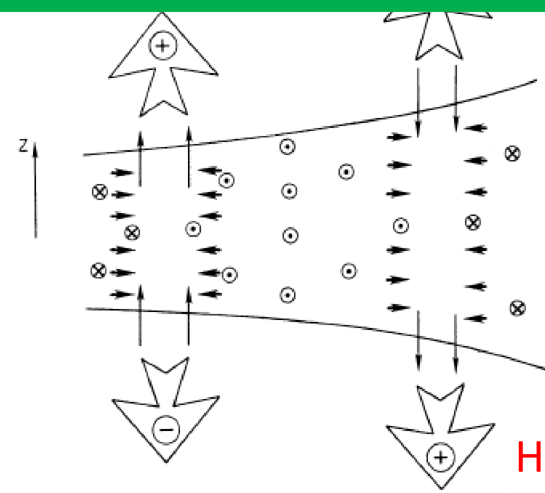

Halo heating and acceleration
→ low energy X, γ, ν

Tajima and Gilden 1987, ApJ 320, 741-745
Haswell, Tajima, and Sakai, 1992, ApJ, 401, 495-507

Anti-correlation of γ flux and spectral index

Blazar: 3C454.3

M ~ 10^9 M_{Sun}

flux

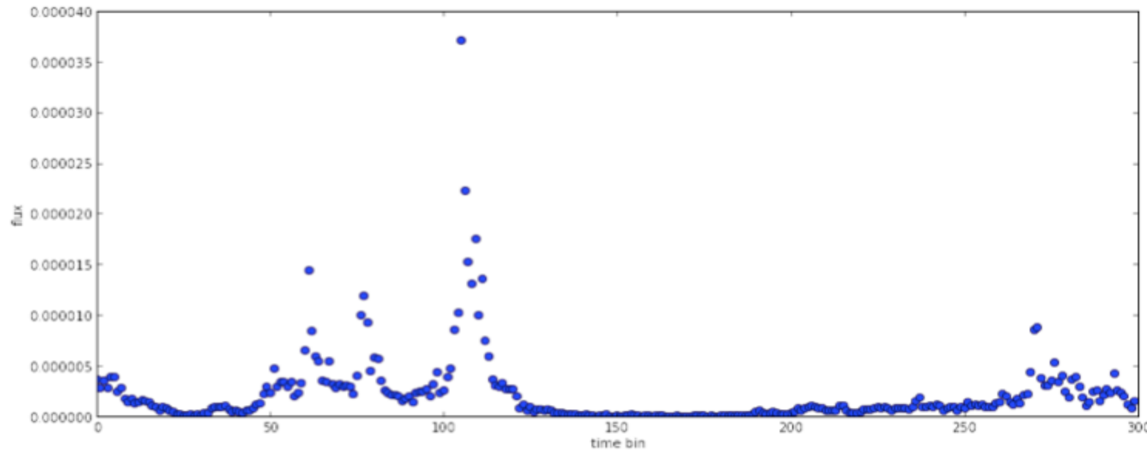

↕ anti-correlate

index

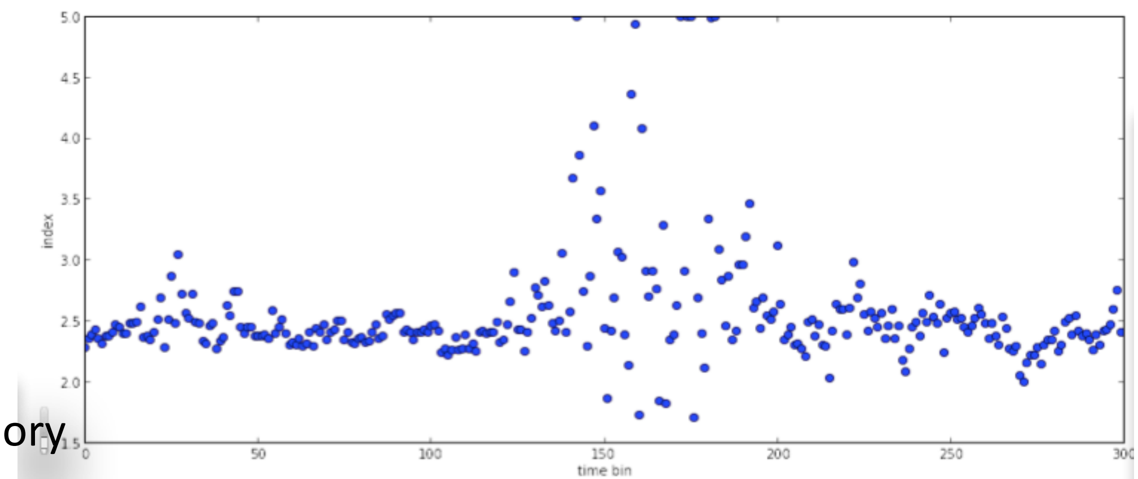

time

N. Canac, et al. MNRAS (2020)

Same anti-correlation as
Blazar AO0235+164

The rise time and burst periods a lot longer (by an order of magnitude)

Quantitative agreement and **correct scaling** with Blazar mass with (broader sense of) Wakefield theory (Ebisuzaki/Tajima)

period ~ *M* ; luminosity ~*M*

Detected **neutrino** from **Blazar**

Neutrino: IceCube-170922A / Blazar: TXS 0506+056

Science **361**, 146 (2020) (…,Barwick,…)

Various γ arriavals

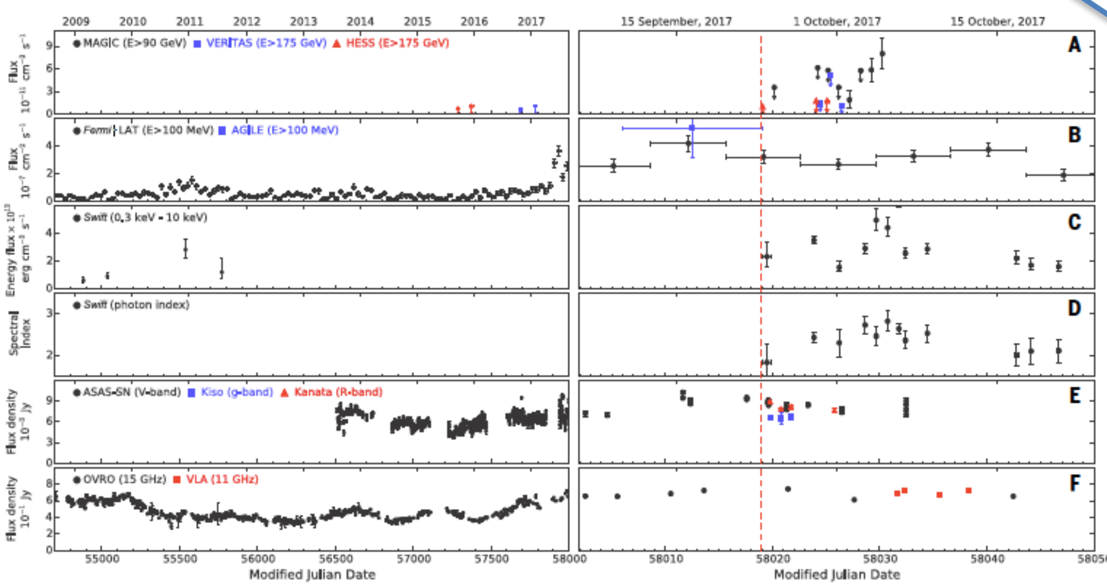

Fig. 3. Time-dependent multiwavelength observations of TXS 0506+056 before and after IceCube-170922A. Significant variability of the electromagnetic emission can be observed in all displayed energy … dashed line marks the detection time of the neutrino IceCube-170922A. The left set of panels shows measurements between MJD 54700 (22 August 2008) and MJD 58002 (6 September 2017). The set of …

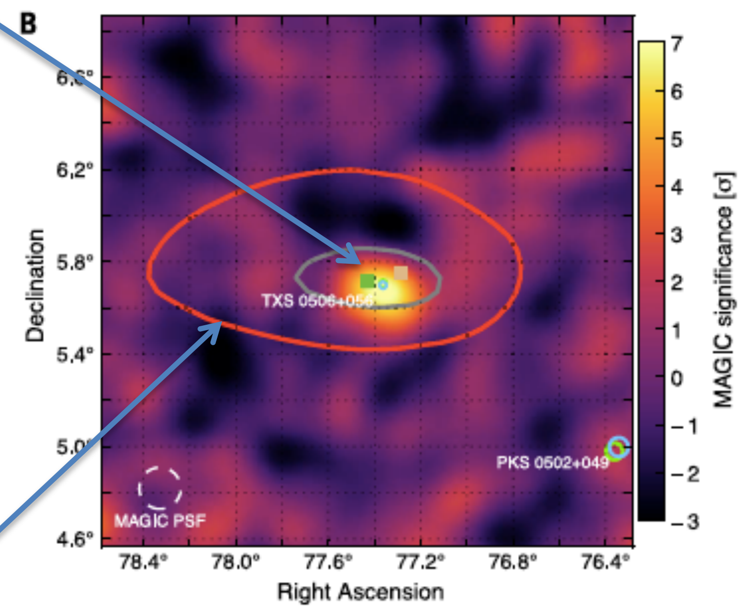

↑

Neutrino arrival

M82: Nearest Starburst Galaxy

M82 X-1: 1000-10000 Ms BH

Just after the collision with M81

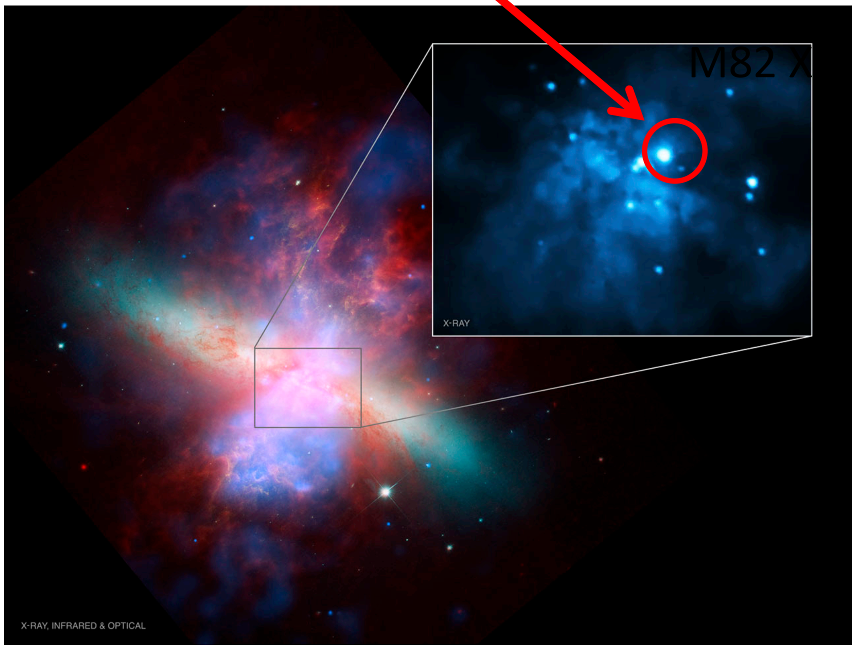

Composite of X-ray, IR, and optical emissions

NASA / CXC / JHU / D. Strickland; optical: NASA / ESA / STScI / AURA/ Hubble Heritage Team; IR: NASA / JPL-Caltech /Univ. of AZ / C. Engelbracht; inset – NASA / CXC / Tsinghua University / H. Feng et al.

TA Hot Spot: UHECRs from M82?

He,Kusenko,Nagataki,… , Phys. Rev. D93, 043011 (2016).

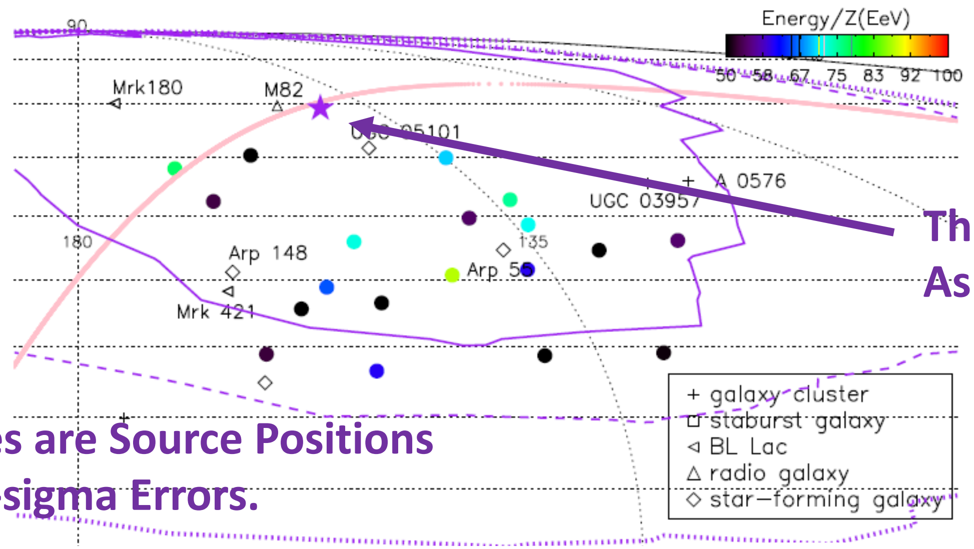

The most likely Source Position As a Result of Our Analysis.

M82 is very Close from the most likely Source Position!

Purple Lines are Source Positions With 1,2,3-sigma Errors.

Source Name	Source Type	Distance (Mpc)	A_1 (°)	A_2 (°)	$P/P_{\rm bes-fit}$ (%)
best-fit	-	-	$17.4^{+17.0}_{-11.0}$	$9.4^{+3.7}_{-0.3}$	100
M82	starburst galaxy	3.4	17.6	9.6	99.8
UGC 05101	star-forming galaxy	160.2	11.6	9.2	96.9
Mrk 180	blazar	185	19.9	9.3	91.3
UGC 03957	galaxy cluster	150.3	14.9	9.5	67.4
A 0576	galaxy cluster	169.0	17.0	9.4	63.4
Arp 55	star-forming Galaxy	162.7	1.9	9.7	55.3
Arp 148	star-forming Galaxy	143.3	10.5	10.0	41.8
Mrk 421	blazar	134	11.2	9.9	35.6

Arrival Direction Map
(cosmic rays>5×10^{19} eV)

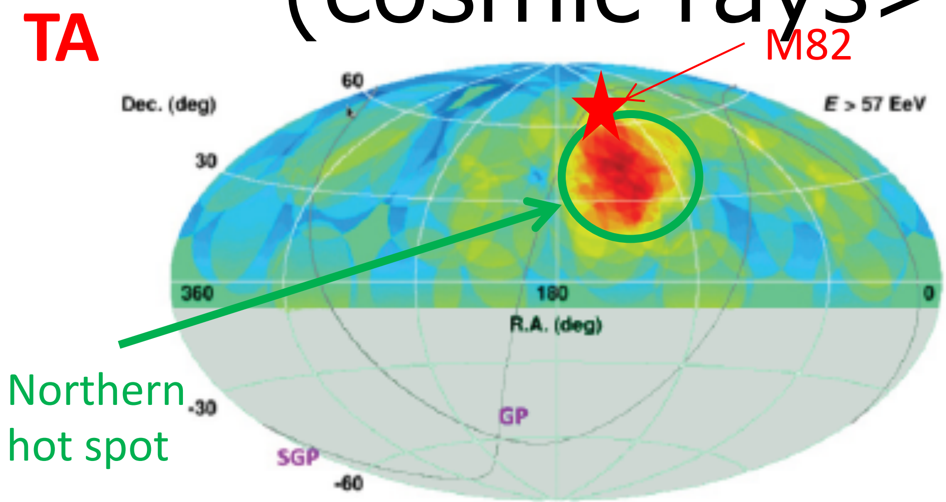

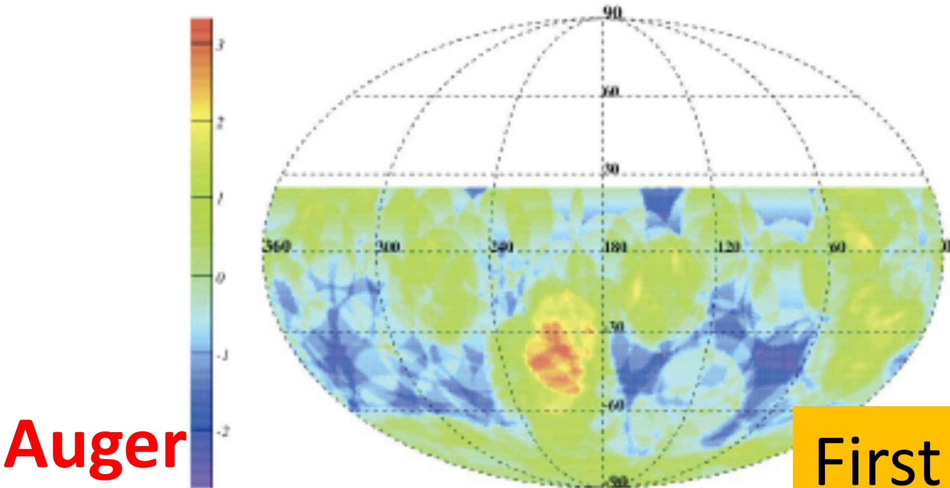

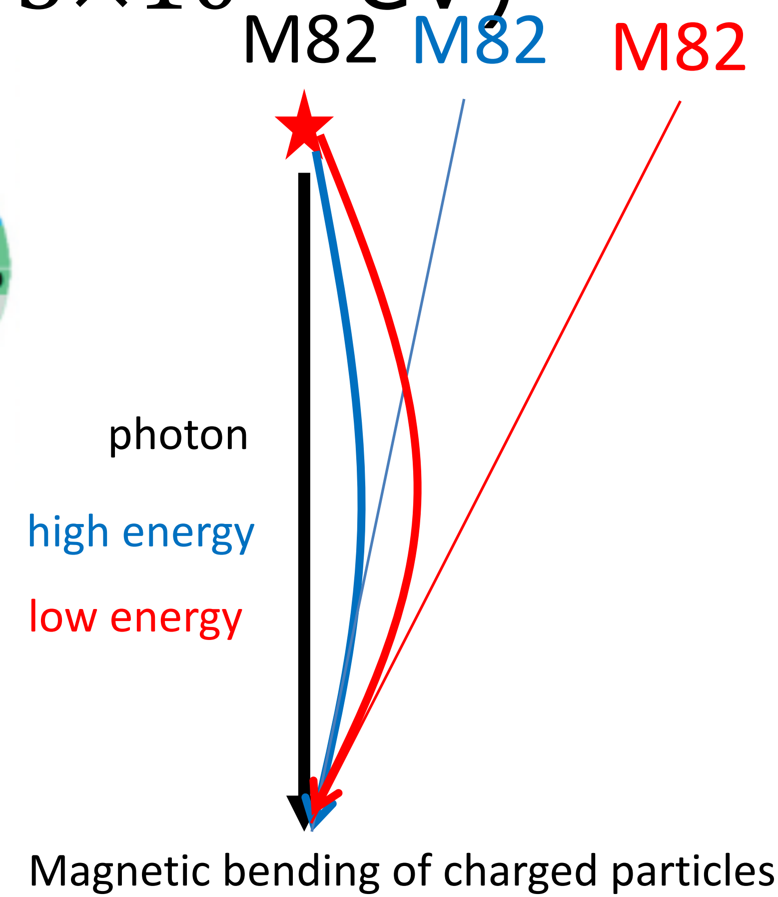

First Identification of CR sources?

First sign of anisotropy in charged particles

An AGN-like Jet in M82?
X-ray/Radio (flare in 1981)

Xu et al. ApJ Letters 799, L28 (2015).

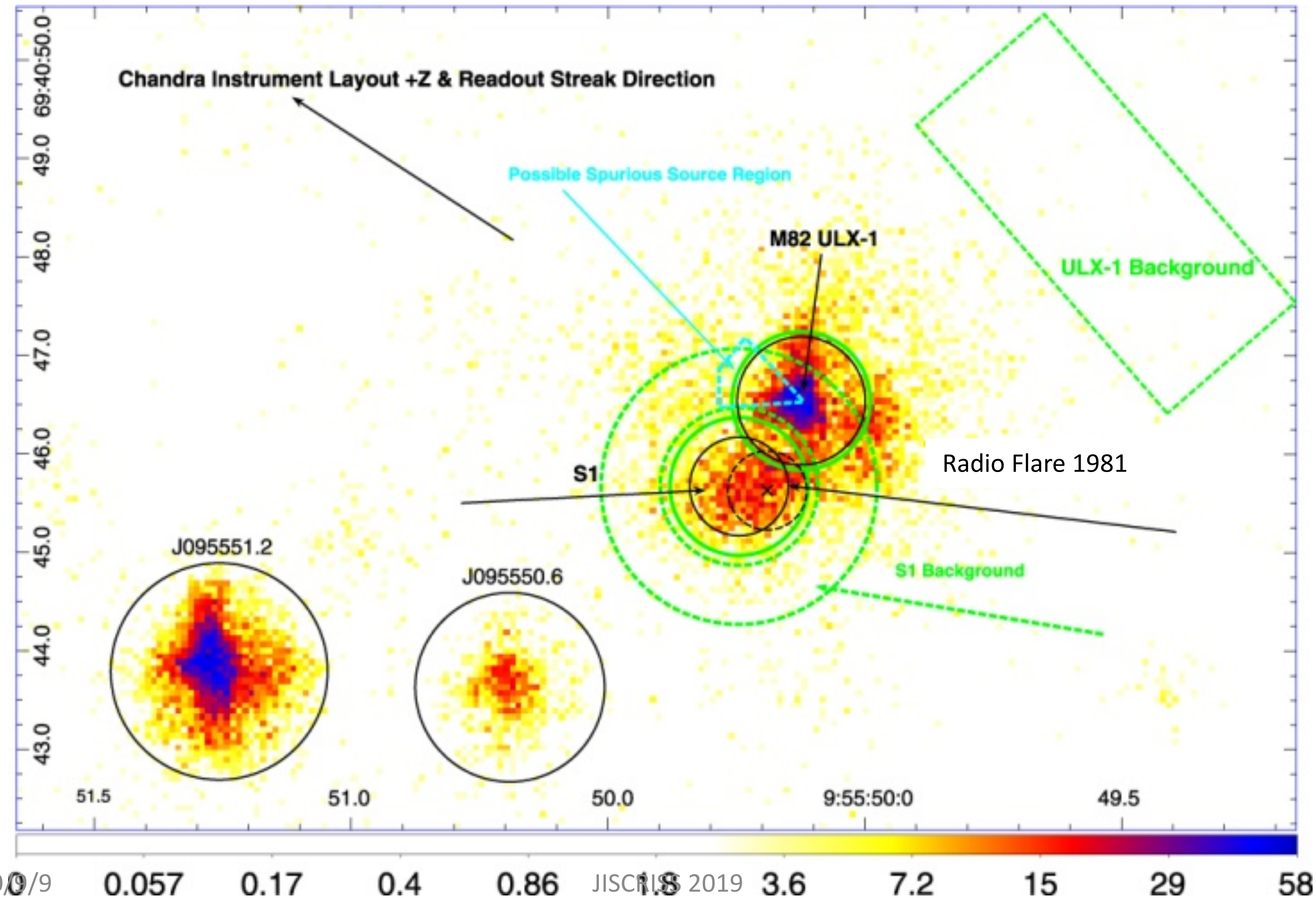

Cen A

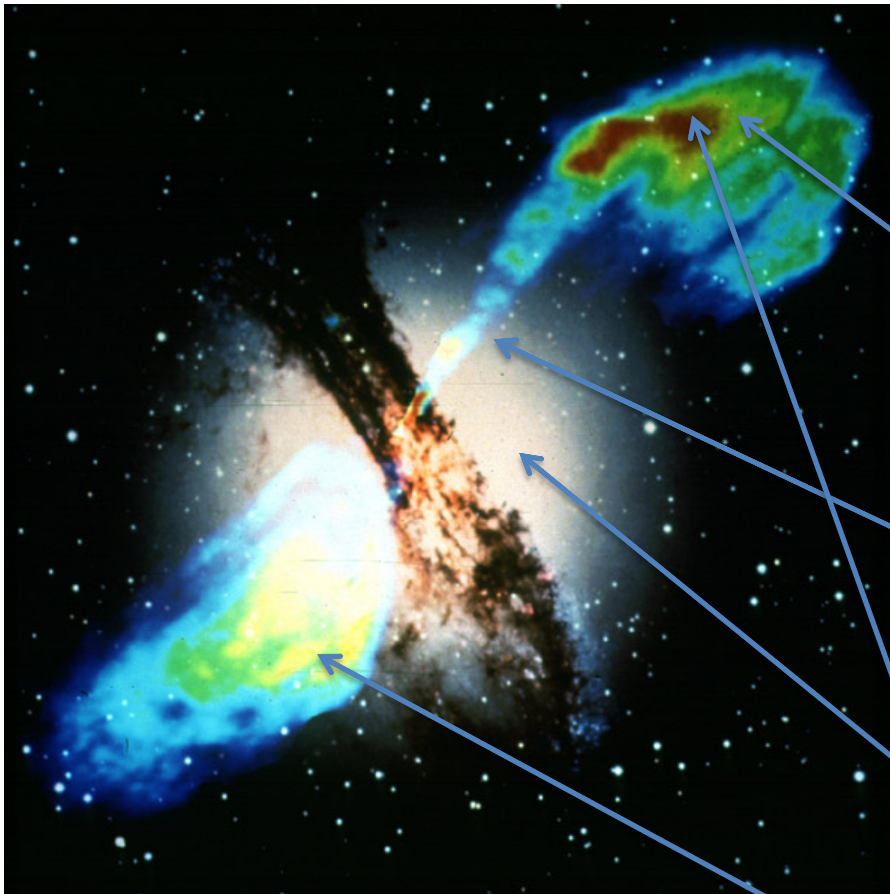

- Distance：3.4Mpc
- Radio Galaxy
  - Nearest
  - Brightest radio source
- Elliptical Galaxy
- Black hole at the center w/ relativistic **jets**, high energy acceleration

Halo emissions

Lobe deceleration of jets

Refs. for Cen A

F. Aharonian; A. G. Akhperjanian; G. Anton; U. Barres de Almeida; A. R. Bazer-Bachi (10 April 2009). "DISCOVERY OF VERY HIGH ENERGY γ-RAY EMISSION FROM CENTAURUS A WITH H.E.S.S.". Astrophysical Journal. 695 (1): L40-L44. --------high energy gamma observation

J. Abraham; P. Abreu; M. Aglietta; C. Aguirre; D. Allard (1 April 2008). "Correlation of the highest-energy cosmic rays with the positions of nearby active galactic nuclei". Astroparticle Physics. 29 (3): 188-204.-------- locale

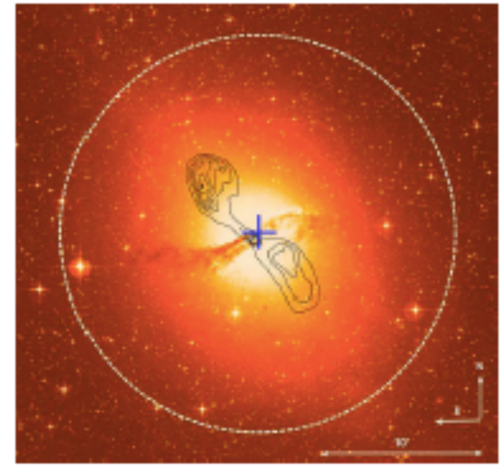

Figure 2. Optical image of Cen A (UK 48 inch Schmidt) overlaid with radio contours (black, VLA, Condon et al. 1996), VHE best fit position with 1σ statistical errors (blue cross), and VHE extension upper limit (white dashed circle, 95% confidence level).

The differential photon spectrum of the source is shown in Figure 3.[36] A fit of a power-law function $dN/dE = \Phi_0 \cdot (E/1\ \mathrm{TeV})^{-\Gamma}$ to the data is a statistically good description ($\chi^2/\mathrm{dof} = 2.76/4$) with normalization $\Phi_0 = (2.45 \pm 0.52_{stat} \pm$

[36] To derive the energy spectrum, a looser cut on the distance to the source is used ($\theta^2 < 0.03\ \mathrm{deg}^2$) to increase the number of photons (the standard cut is $\theta^2 < 0.015\ \mathrm{deg}^2$).

No. 1, 2009 DISCOVERY OF VHE γ-RAY EMI

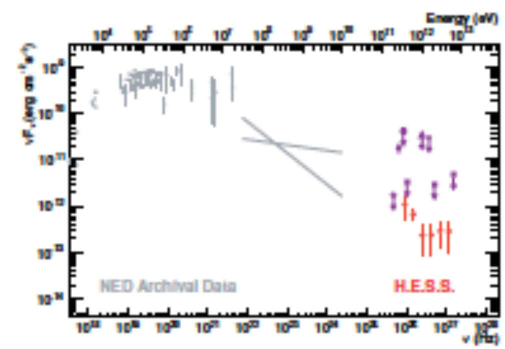

Figure 4. SED of Cen A. Shown are the VHE spectrum as measured by H.E.S.S. (red filled circles), previous upper limits and tentative detections in the VHE regime (purple markers; Grindlay et al. 1975: open diamond; Carraminana et al. 1990: open cross; Allen et al. 1993: filled circle; Rowell et al. 1999: open triangle; Aharonian et al. 2005: open circle; Kabuki et al. 2007: filled squares), EGRET measurements in the GeV regime (Sreekumar et al. 1999: gray bow tie), and data from the NASA Extragalactic Database (NED; gray filled circles).

NGC253

ı from our survey of X-ray sources in NGC 253 (Barnard et al. 2008b). For
ned by the source detection routine; these have uncertainties of ~2 arcsec.
ı and MOS detectors. Next, we give the details of the best-fitting spectral
Γ) and photon index (Γ), along with the corresponding χ^2/d.o.f. and 0.3–
heses indicate 90 per cent confidence limits on the final digit.

OS	$N_H/10^{21}$ atom cm^{-2}	kT/keV	Γ	χ^2/d.o.f.	$L/10^{39}$
90	2.00(2)	0.73(5)	2.14(4)	347/323	2.90(12)
14	2.9(2)	0.98(6)	1.94(5)	374/374	4.10(19)
56	6.0(11)	0.94(8)	3.4(5)	84/76	2.4(4)

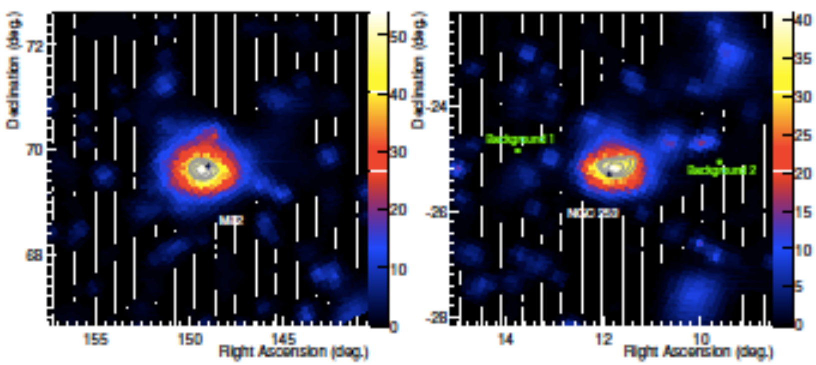

Figure 1. Test statistic maps obtained from photons above 200 MeV showing the celestial regions (6° by 6°) around M82 and NGC 253. Aside from the source associated with each galaxy, all other *Fermi*-detected sources within a 10° radius of the best-fit position have been included in the background model as well as components describing the diffuse Galactic and isotropic γ-ray emissions. Black triangles denote the positions of M82 and NGC 253 at optical wavelengths; gray

top of
QPOs
ver-law
08 X-1
7).
udy of
vations
power
C 1313
others
l upper
hat the

y spec-
power
ons on
dstone,
xcess',
l com-
andard
by the
2006).
Newton
r EPIC
r and a
e inner
excess
disc +
wever,

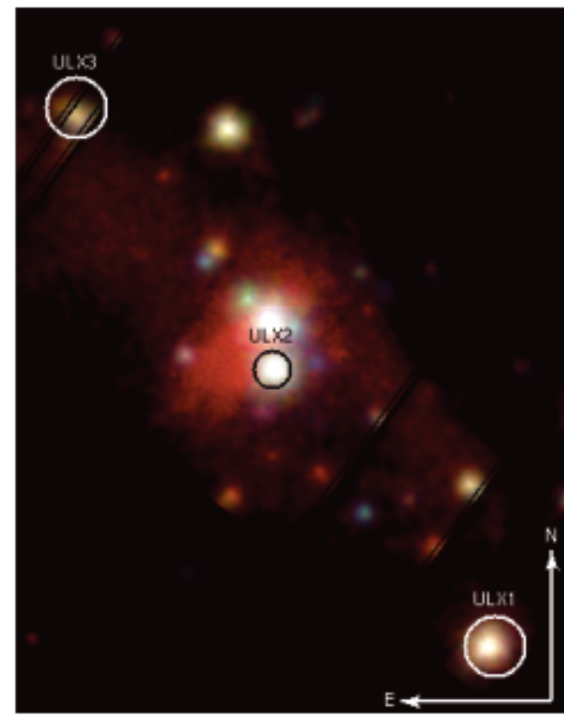

Figure 1. Detail of a three colour pn + MOS image of NGC 253 showing ULX1, ULX2 and ULX3. Red represents 0.3–2.0 keV, green represents 2.0–3.0 keV, and blue represents 4.0–10 keV. The image is log-scaled, and the source extraction regions for the ULXs are labelled.

NGC 0253: Starburst galaxy

Gamma emission:

Abdo et al. 2010, Detection of gamma-ray emission from the starburst galaxies M82 and NGC253 with the Large Area Telescope on FERMI, Astrophys. J. Letters, L152-L157.

X-ray source found:

R. Barnard, 2010, In-depth studies of NGC253 ULXs with XMM-Newton: remarkable variability in ULX1, and evidence for extended coronae, Mon. Not. Roy. Soc, 404, 42-47.

SS 433: Microquasar

Gammaray energy ~ 10TeV Abeysekara, et al. (2018)

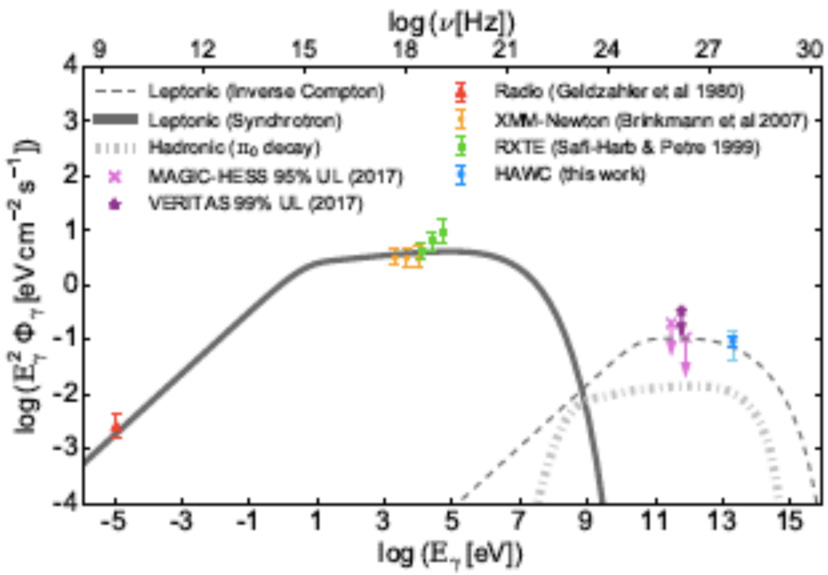

Figure 2: **Broadband spectral energy distribution of the eastern emission region.** The data include radio [18], soft X-ray [12], hard X-ray [16], and VHE γ-ray upper limits [19,20], and HAWC observations of e1. Error bars indicate 1σ uncertainties, with the thick (thin) errors on the HAWC flux indicating statistical (systematic) uncertainties and arrows indicating flux upper limits. The multiwavelength spectrum produced by electrons assumes a single electron

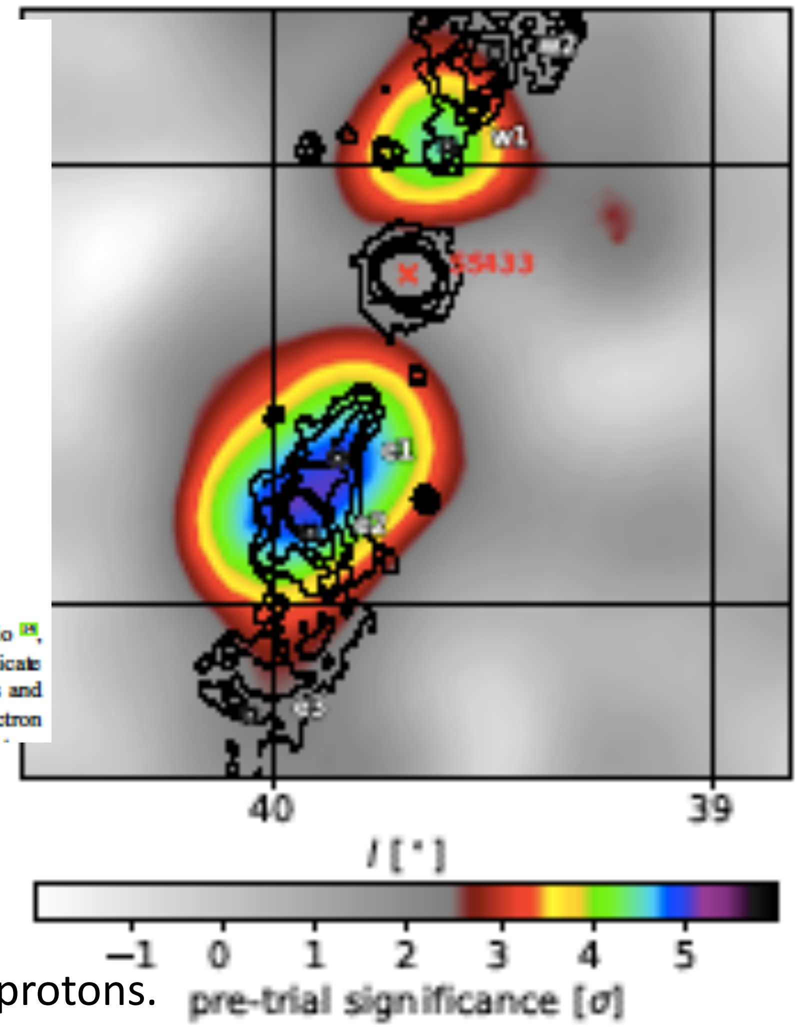

[Wakefield proton theory:

could go as high as 3×10^{19} eV]: Can we observe?

galactic center's dense plasma and B might affect protons.

SS433 precession jets